Universal Journal of Public Health 10(2): 226-240, 2022
DOI: 10.13189/ujph.2022.100209 http://www.hrpub.org

Compendium of Tunable Data-driven Approaches for Smoothing Parameter Learning for Kernel Density-based Normal Systolic Blood Pressure Detection

David Kwamena Mensah, Francis Eyiah-Bediako, Samuel Assabil*

Department of Statistics, University of Cape Coast, Ghana

*Corresponding Author: dmensah@ucc.edu.gh

Received December 1, 2021; Revised March 22, 2022; Accepted April 15, 2022

Cite This Paper in the following Citation Styles

***(a)**: [1] David Kwamena Mensah, Francis Eyiah-Bediako, Samuel Assabil, "Compendium of Tunable Data-driven Approaches for Smoothing Parameter Learning for Kernel Density-based Normal Systolic Blood Pressure Detection," Universal Journal of Public Health, Vol.10, No.2, pp. 226-240, 2022. DOI: 10.13189/ujph.2022.100209*

***(b)**: David Kwamena Mensah, Francis Eyiah-Bediako, Samuel Assabil, (2022). Compendium of Tunable Data-driven Approaches for Smoothing Parameter Learning for Kernel Density-based Normal Systolic Blood Pressure Detection. Universal Journal of Public Health, 10(2), 226-240, DOI: 10.13189/ujph.2022.100209*

Abstract The performance of a Kernel density-based approach for the detection of normal physiological vital signs can be affected drastically by the smoothing parameter that controls the underlying density. As a result, its application in practical (critical) areas such as public health, clinical trials and digital therapeutics (DTx), require some modifications for accurate and intelligent decisions. In this regard, this paper introduces a compendium of novel tunable data-driven smoothing parameter statistics together with tuning schemes for detecting normal systolic blood pressure (SBP) observations from continuously monitored SBP data. The tuning is designed based on both the entire data and observation-specific levels, using statistics that are by-products of the developed detector model, thereby allowing the smoothing parameters to adapt appropriately to the dynamics of the SBP data. A real systolic blood pressure data application illustrates the utility of the proposals, with significant improvement in overall performance over its well-known counterparts, the smoothed cross-validation bandwidth selector (HSCV), normal scale bandwidth selector (Hns), and Plug-in bandwidth selector (Hpi), implemented in standard statistical packages such as R. In particular, it turns out that observational-level tuning of smoothing parameters ensure better improvement in detection performance over the entire data tuning. Though performance assessment focused on accuracy, various problem-specific detection solutions can be designed for use in some application areas such as the pharmaceutical industries. For example, solution(s) based on sensitivity and specificity can be considered for early-stage clinical trials, for which several tuning proposals are evidently up to the task.

Keywords Smoothing Parameter, Data-based Tuning, Kernel Density Function, Moment, Systolic Blood Pressure

1 Introduction

Physiological vital signs monitoring has gain popularity in healthcare, in many hospitals around the globe due to its fundamental link with the condition of health. Physiological vital signs can be viewed as performance measurements from vital organs of the human body. Usually, deterioration in health manifests in the physiological vital signs either jointly or individually. Thus, subtle changes in these vital signs are key to the identification of indicators of early signs of deterioration [1, 2]. As a result, monitoring systems have been considered over the years, based on the principle of tracking deterioration in health via vital signs. Key examples are the track and trigger and its modified versions, where vital signs observations of patients or subjects are periodically monitored and compared with their corresponding normal ranges using early warning scores (EWS) [3, 4]. Patients are prioritized for review under this scheme when pre-defined normal thresholds are exceeded by the EWS based on the sum or otherwise.

Novelty detection provides another appealing alternative for

monitoring health within the model-based framework. Here, the identification of deterioration in health is achieved via the deviation of data pattern from a normal pattern defined by an assumed normality model [5]. For a comprehensive review on novelty detection approaches to vital signs monitoring, see, for example, [6] and [7]. The utility of novelty detection for monitoring gastro-intestinal post-operative patients has been explored within the Kernel density context, see for example, [8]. The physiological trajectory of normal recovery was based on data from normal patients. Also, [9] applied kernel density-based novelty detection to physiological vital signs of chronic obstructive pulmonary patients to prioritize them for clinical review. Cumulative distribution functions of vital signs were employed to set normal thresholds. It turns that novelty detection monitoring systems perform better when the normal model is available or correctly determined from an assumed normal data set. Nevertheless, the availability of normal data cannot be guaranteed for all data-generating systems at all times. There are certain situations that may define new normal patterns or change the system manifestations yielding entirely unknown data patterns. One practical example of such a situation is a pandemic, for example, the "COVID 19" pandemic.

The impact of the "COVID 19" pandemic on every facet of the economy of every country is clearly evident, especially, on healthcare. Consequently, treatment and monitoring of patients nowadays are marred by the pandemic associated challenges such as lack of human interaction, a key tool for seeking effective solutions to problems. This suggests, renovating or tuning existing structures to adapt appropriately to the defining patterns orchestrated by the pandemic. In the case of health monitoring through physiological vital signs, the issue of mining required normal data patterns directly from available data becomes apparently clear. In this regard, [10] considered a nonparametric approach based on kernel density for detecting normal systolic blood pressure using continuously monitored systolic blood pressure data. The detector model was based on statistics obtained from the probability density function of the data using the idea of moments of probability distributions. The probability density function of the data was estimated via Kernel density estimation. Also, the smoothing parameter utilized in the kernel density estimation was tuned by a deterministic parameter α_0 which had its values set by the possible candidate values of one of the defining statistics of the normal detector model. Their approach yielded an overall detection accuracy of 98%.

The probability distribution of empirical data provides standard source for underscoring important features underlying the data in a fast way. As a result, it serves as one of the key elements of many modeling frameworks [10]. Kernel method of density estimation is one of the powerful nonparametric techniques for gaining insight into data [11]. This has led to its wide spread application in several areas of practical importance, see, for example, [12], [13], [14], [15], [16], [17], and [10].

Practical implementation of kernel density method requires that an appropriate smoothing parameter is selected. This parameter has the potential to cause deficient smoothing, leading to rough density estimates that are characterized with spurious features that are artifacts of the sampling process. On the other hand, vital features characterizing the underlying structure in the data can be smoothed out with a smoothing parameter that yields excessively smoothed density estimates [11]. With the above observations, it becomes relatively easy to envision the impact of smoothing parameters on the performance of kernel density estimators and their related models, especially in statistical problems with practical inferential implications. Examples of scientific fields with such problems are public health, medicine, and industrial processes.

The performance of a kernel density estimator is well known to be determined largely by the choice of smoothing parameter and slightly by the choice of the kernel function [12, 18]. Due to this, the selection of smoothing parameter for kernel density estimation has received much attention in the literature, particularly, in the case of univariate kernel density estimation, see for example, [19], [20], [21], and [22]. [11] provides a comprehensive survey of "first-generation" and "second-generation" smoothing parameter selection methods for one-dimensional kernel density estimation.

Although, a broad range of smoothing parameter selectors exists, making the kernel density approach attractive in many fields of applications, its direct application is challenged in some practical areas such as public health, digital therapeutics (DTx), medicine, and industrial process control, where inferential decisions can impact directly on humanity either positively or negatively. More importantly, in health monitoring, an aspect of public health that hinges on physiological vital signs monitoring, the above challenges can be amplified due to the complex nature of physiological vital signs and their relationship with several other health-related factors. The ability of a smoothing parameter to explore the dynamics of data is vital in allowing better adaption, resulting in the density function being well estimated. This is key for data set exhibiting functional patterns instead of linear, like the one considered in this paper.

In this paper, we build on the work of [10], focusing on self-normal detection in one-dimensional physiological vital signs. In particular, we consider systolic blood pressure, one of the key components of blood pressure (BP) monitoring systems [2]. Systolic blood pressure can be defined as the amount of pressure created in the arteries when the heart muscle contracts. Though, the approach of [10] is an appealing premier proposal for mining appropriate normal SBP, it offers only a single deterministic way for tuning an assumed smoothing parameter. We consider a compendium of novel data-based smoothing parameters that can be tuned at both the observation level or entire data level, using by-products of the assumed detector model, for mining normal SBP from continuously monitored SBP measurements. Tuning the smoothing parameters enable them to adapt to the underlying

features of the data, leading to improved performance of the developed detector. For the SBP data with the likelihood of high variability, a tuned smoothing parameter may not yield an over-smoothed or under-smoothed density function for the development of appropriate self-normal detectors.

The rest of the paper is structured as follows. Section 2 outlines the proposed statistical methods. Section 3 details the implementation protocols assumed for the proposed methods. In Section 4, performance assessments adopted are briefly discussed and a real data application implemented to illustrate the utility of the proposed statistical methods. Finally, Section 5 concludes.

2 Methods

2.1 Kernel density-based normal systolic blood pressure detector

Let $f(y;h)$ denotes the probability density function for sample systolic blood pressure observations, $y_1, y_2, \ldots, y_n$, where h is an unknown parameter. Let $\hat{f}(y;h)$ be the estimator of $f(y;h)$. Then, normal structures underlying the systolic blood pressure data can be detected empirically based on the statistic, $S(y,\tilde{f})$ [10]

$$S(y,\tilde{f}) = g\Big(\tilde{f}_{\hat{f},\tilde{m},y}\Big)y, \tag{1}$$

$$g\Big(\tilde{f}_{\hat{f},\tilde{m},y}\Big) = \frac{\phi_1\Big(\tilde{f}_{\hat{f},\tilde{m}},y\Big)}{\sigma_1},$$

where $\phi_1\Big(\tilde{f}_{\hat{f},\tilde{m}},y\Big) = \tilde{f}_{\hat{f},\tilde{m}} - y, \tilde{f}_{\hat{f},\tilde{m}} = \frac{-\log\hat{f}}{\tilde{m}}$, $\hat{f} = \hat{f}(y;h)$. Also, the statistics σ_1, and $\tilde{m}$ are the standard deviation and median of $\phi_1\Big(\tilde{f}_{\hat{f},\tilde{m}},y\Big)$ and $-\log\hat{f}$ respectively. Note that $\hat{f}(y;h)$ is obtained by evaluating (2) for each y_i for $i = 1, 2, \ldots, n$ conditioned on the entire data y and h

$$\hat{f}\Big(y_i \mid y,h\Big) = \frac{1}{n}\sum_{j=1}^{n}\frac{1}{\sqrt{2\pi h^2}}\exp\Big(-\frac{(y_j-y_i)^2}{2h^2}\Big). \tag{2}$$

For detailed information on nonparametric approach to Kernel density estimation and its application in physiological vital signs modeling see for example [23], [24], and [8]. The possible values of the statistic, $S(y,\tilde{f})$, particularly, the positive ones, $S(y,\tilde{f}) \geq 0$ are informative on likely candidates that naturally mimic the normal pattern manifested by the systolic blood pressure measurement. Thus, various appealing detection thresholds can be considered apart from the natural lower bound value of 0, depending on the interest of the detection problem.

2.2 Smoothing parameter for normal SBP detection

2.2.1 Data-driven estimators with common weights

The proposals considered here are based on the principle that each observation contributes significantly to the common pattern underlying the data. The following commonly weighted estimators are considered.

$$h^{\delta}_{c_1} = \frac{\delta}{n}\sum_{i=1}^{n}\omega_{1i} \tag{3}$$

where $\omega_{1i} = \frac{1}{10}\sum\limits_{j\in\{\text{KNNs}\}}(y_i - y_j)^2$.

$$h^{\delta}_{c_2} = \sqrt{\frac{\delta}{n}\sum_{i=1}^{n}\omega_{2i}}, \omega_{2i} = \frac{1}{m}\sum_{j=1}^{m}\Big(y_i - y_j\Big)^2 \tag{4}$$

$$h^{\delta}_{c_3} = \sqrt{\psi(z_{1i})}, z_{1i} = \delta\omega_{1i} \tag{5}$$

$$h^{\delta}_{c_4} = \sqrt{\psi(z_{2i})}; z_{2i} = \delta\omega_{2i}, \tag{6}$$

where $m = (n-1), y_j = y_{(-i)}$ and $\psi(x)$ function computes the Orthogonalized Gnanadesikan-Ketterning (OGK) statistic [25, 26] for a single-variate sample set $x = [x_1, x_2, \ldots, x_n]$ generated from a distribution with mean μ and variance σ^2.

$$\psi(x) = \frac{\sum\limits_{i=1}^{n}x_i\eta(\omega_i)}{\sum\limits_{i=1}^{n}\eta(\omega_i)}, \omega_i = \frac{x_i - \tilde{\mu}_0}{\tilde{\sigma}_0}, \tag{7}$$

where $\eta(x) = [1 - t_{x,a}]^2\,\mathrm{I}_{(|x|\leq a)}, t_{x,a} = (\frac{x}{a})^2, a = 4.5$, $\tilde{\mu_0}$ and $\tilde{\sigma}_0$ are the median and median absolute deviation (MAD) of x.

The estimator in (3) is an adapted version of the average localized distance proposal of [27] in one-dimension. The deterministic parameter, δ, is termed a tuning parameter, and in this case, it is assumed non-adaptive or common to all observations. It serves the basic function of ensuring that estimate obtained adapt properly to the underlying physiological pattern by avoiding under-smoothing or over-smoothing of vital features of the data.

2.2.2 Data-driven estimators with adaptive weights

Allowing each observation to propose a candidate weight according to its contribution in terms of some similarity measure leads to alternative data-driven estimators with adaptive weights. We consider the following set of statistics with adaptive data tuning property.

$$h^{1}_{v} = \sqrt{\frac{1}{n}\sum_{i=1}^{n}\delta^{v}_{1i}\omega^{2}_{1i}}, \tag{8}$$

where ω_{1i} is as defined in (3).

$$h_v^2 = \sqrt{\frac{1}{n}\sum_{i=1}^{n}\delta_{2i}^v\omega_{2i}}, \tag{9}$$

$$h_v^3 = \sqrt{\frac{1}{n}\sum_{i=1}^{n}\lambda\left(\delta_{2i}^v\right)s_1\left(\omega_{2i}\right)}, \tag{10}$$

where $\lambda(x) = \sqrt{x}$.

$$h_v^4 = \sqrt{\psi(\delta_{3i}^v s_2\left(\omega_{2i}\right))}, \tag{11}$$

where $s_2(\omega_{2i})$ and $s_1(\omega_{2i})$ are similarity statistics given in Subsection 2.3.

2.3 Automatic data-driven choices for δ

Let $s_2(\omega_{2i})$ and $s_1(\omega_{2i})$ denote similarity statistics with the following definitions.

$$s_2\left(\omega_{2i}\right) = \sqrt{\sum_{j=1}^{n-1}\left(\omega_{2j}-\omega_{2i}\right)^2}$$

$$s_1\left(\omega_{2i}\right) = \sqrt{\sum_{j=1}^{n-1}|(\omega_{2j}-\omega_{2i})|},$$

where $\omega_{2j} = \omega_{2i}[-i], i = 1, \ldots, n$. Then the following similarity vectors results upon evaluating the above statistics at ω_{2i} for $i = 1, 2, \ldots, n$.

$$s_2 = \left[s_2(\omega_{21}), s_2(\omega_{22}), \ldots, s_2(\omega_{2n})\right]$$

$$s_1 = \left[s_1(\omega_{11}), s_1(\omega_{12}), \ldots, s_1(\omega_{1n})\right]$$

respectively. Define the median of s_2 and s_1 respectively as $\tilde{s}_2$ and $\tilde{s}_1$ respectively. The corresponding minimum values can be denoted by s_2^m and s_1^m. Based on the above statistics, we consider the following data-driven choices for δ.

$$\delta_g = \alpha, 0.1 < \alpha \leq 1,\ \delta_1 = \frac{1}{\sqrt{\alpha_g s_2^m}}$$

$$\delta_2 = \frac{1}{\alpha_g\sqrt{s_2^m}},\ \delta_3 = \frac{1}{\sqrt{\tilde{s}_1}},\ \delta_4 = \frac{1}{\sqrt{h(s_2)}}$$

$$\delta_5 = \frac{\vartheta(y')}{\vartheta(y)}, \delta_6 = \begin{cases}\gamma\left(\tilde{y}, y_{max}\right) - 1, & \text{if } \tilde{y} > y_{max}\\ 1-\gamma\left(\tilde{y}, y_{max}\right), & \text{if } \tilde{y} < y_{max},\end{cases}$$

$$\delta_7 = \frac{1}{\sqrt{\xi}}, \xi = \frac{y_{max}-y_{min}}{6} \tag{12}$$

where

$$\gamma\left(x_1, x_2\right) = \frac{x_1}{x_2},\ y_{max} = max\{y_1, y_2, \ldots, y_n\},$$

$y' = \{y \geq \tilde{y}\}$, and $\tilde{y}$ denotes the median of the vector y. The function $\vartheta(z)$ computes the number of elements in the vector z.

2.4 Automatic data-driven choices for $\delta_{1i}^v, \delta_{2i}^v$ and δ_{3i}^v

Adaption of the smoothing parameter based on observation-specific locations may allow easy learning of the underlying dynamics of the systolic blood pressure trend. This is because physiological features can be very dynamic depending on several factors. Particularly, the position of systolic blood pressure observation in relation to the rest of the observations is fundamental to decide whether a given observation follows a common pattern determined by the physiological features of the underlying data. In this regard, we propose allowing each observation to direct an appropriate tuning based on its proximity or relationship with the other observations. Thus, we introduce observation-level choices for δ based on the following statistics.

$$\delta_i^1 = \frac{1}{\sqrt{\delta_g m s_2(\omega_{2i})}},\ \delta_i^2 = \frac{1}{\delta_g\sqrt{m s_2(\omega_{2i})}}$$

$$\delta_i^3 = \frac{1}{\delta_g\sqrt{m s_1(\omega_{2i})}},\ \delta_i^4 = \frac{1}{\sqrt{\delta_g m s_1(\omega_{2i})}}$$

$$\delta_i^5 = \frac{1}{s_2(\omega_{1i})},\ \delta_i^6 = \frac{1}{\sqrt{s_2(\omega_{1i})}},\ \delta_i^7 = \frac{1}{\sqrt{s_2(\omega_{2i})}}$$

$$\delta_i^8 = \frac{\vartheta(y_j^a)}{\vartheta(y)},\ \delta_i^9 = \frac{\vartheta(y_j^b)}{\vartheta(y)},\ \delta_i^{10} = \frac{\delta_i^8+\delta_i^9}{2}, \tag{13}$$

where $y_j^a = \{y > y_i\}, y_j^b = \{y < y_i\}$ and y_j denotes the subset of observations without the ith observation.

2.5 Expected value contribution-based choice for δ, δ_{1i}^v and δ_{2i}^v

Interesting features of random variables can be assessed via the probability distribution function or model assumed for such random variables. This assessment can be achieved based on some fundamental statistics of the probability distribution function such as the moments. We propose the use of moment-based information for derivation of both common and observation-specific data tuning values for learning data-driven smoothing parameters for normal systolic blood pressure detection.

Consider the first non-central population moment as an empirical measure of center for a random variable, say, Y, following the probability distribution with density function, $f(y)$, where the parameter dependencies are suppressed

$$\mu_y = \mathrm{E}\Big[Y\Big] = \int_y yf(y)dy. \tag{14}$$

Let $c(y) = yf(y)$. Then, it is straightforward to observe the role of $c(y)$ as a measure of the contributions of observations in the random sample. With the density values $f(y)$, as weights, random variables in the sample contribute differently to the common center, $\mathrm{E}\Big[Y\Big]$. The spatial locations of the observations under the probability density function are fully captured in $c(y)$. The automatic control for outlying observation characteristic of the density weights is clearly evident with observations close to the center having more impact than those which

are at some appreciable distances from the center. This feature is inherited by the statistic, $c(y)$, automatically. Thus, $c(y)$ becomes an appealing source for deriving data-driven tuning statistics for performing automated normal systolic blood pressure detection. Based on the above observation, we consider the following expected value contribution-based selection procedures for δ and δ_i^v.

It is important to note that some tuning parameters yield vectors whiles others results in matrices. In particular, all tuning parameters dependent on δ_g generate a matrix of values with dimensions inherited from δ_g and the data considered. The calibration is such that each value of δ_g gives a vector of observation-level tuners that is able to capture the dynamics associated with the observation in relation with the others, based on a given proximity (similarity) measure.

$$\delta_8 = \frac{min\left(\tilde{\mu}^c, \mu_c^{max}\right)}{max\left(\tilde{\mu}^c, \mu_c^{max}\right)},\ \delta_9 = \frac{1}{\sqrt{\mu_c^{max} - \mu_c^{min}}},$$
$$\delta_i^{11} = \frac{c(y)}{\mu_c^{max}},\ \delta_i^{12} = \frac{1}{\sqrt{\frac{\omega_{2i}}{\tilde{\mu}_c}}},$$
$$\delta_i^{13} = \frac{1}{\sqrt{n\alpha_g s_1\left(c(y_i)\right)}},\ \delta_i^{14} = \frac{1}{\sqrt{n\alpha_g s_2\left(c(y_i)\right)}}, \quad (15)$$

where $\tilde{\mu}^c, \mu_c^{max}$ and μ_c^{min} are the median, maximum and minimum values of the contribution statistic, $c(y)$. Based on the above proposals, we outline the possible candidate choices for δ_{1i}^v and δ_{2i}^v explicitly. For δ_{1i}^v, the applicable candidates among the δ_is are δ_i^8, δ_i^9 and δ_i^{12}. In the case of δ_{2i}^v, $\delta_i^1, \delta_i^2, \delta_i^3, \ldots, \delta_i^7, \delta_i^{13}$ and δ_i^{14} can be used. The δ_{3i}^v can admit $\delta_i^1, \delta_i^2, \delta_i^3, \ldots, \delta_i^8, \delta_i^{13}, \delta_i^{14}$.

3 Implementation

We follow the probability density function (PDF) based proposals for detecting appropriate normal systolic blood pressure (SBP) trend from training data by [10] in assessing the current proposals for data-driven smoothing parameters learning for normal SBP detection. In particular, the double-fit PDF scheme is considered. We briefly summarize the above scheme before applying it. The basic idea is that the underlying probability density function of the training data is estimated and then utilized twice as pre-processing tool and detector. The key steps involved in the above scheme are outlined below.

(a) Estimate the pdf of the data y using model (2).

(b) Derive pdf based statistics

$$v_i = \frac{1}{y_i}\sum_{j=1}^{N} \hat{f}(y_i \mid y_j, h)$$
$$\tilde{\mu} = \text{median}\left[v(y)\right]$$

where $v = [v_1, \ldots, v_n]\,,\ y_j = y_{(-i)}$.

(c) Find y^*, such that $y^* = (y < \tilde{\mu})\,.$

(d) Estimate the pdf of y^* with model (2)

(e) Apply model (1) to results obtained.

The implementation of the above steps, especially step (b) used each of the proposals for h. Particularly, in estimating the density of the data using (2), h was set to each of $\hat{h}_{c_1}^{\delta}, \hat{h}_{c_2}^{\delta}, \hat{h}_{c_3}^{\delta}$ and $\hat{h}_{c_4}^{\delta}$. Furthermore, the density estimation using observational-level tuning specific estimators of h, h^2 was considered for each of h_v^1, h_v^2, h_v^3 and h_v^4. True annotated systolic blood pressure data is compared with algorithmic annotations for the computation of performance statistics.

4 Performance Assessment

We consider for assessment of performance, the most commonly used performance assessment measures for binary classifiers. These measures are introduced in brief here using contingency Table 1 for simplicity. We adopt the following notations. TP = True Positive, FN = False Negative, TN = True Negative, and FP = False Positive.

	True situation	
Predicted situation	Positive	Negative
Positive	TP	FP
Negative	FN	TN

Table 1. A 2×2 contingency table for a generic binary classifier

The sensitivity of a binary detector can be defined as the fraction of the actual positives that are correctly identified by the detector. On the other hand, the specificity represents the fraction of the actual negatives that the detector identified correctly.

$$\text{SS} = \frac{\mathcal{N}(TP)}{\mathcal{N}(TP) + \mathcal{N}(FN)} \quad (16)$$

$$\text{SP} = \frac{\mathcal{N}(TN)}{\mathcal{N}(TN) + \mathcal{N}(FP)}. \quad (17)$$

The accuracy (ACC) of the detector can be defined as

$$\text{ACC} = \frac{\mathcal{N}(TP) + \mathcal{N}(TN)}{\mathcal{N}(TP) + \mathcal{N}(TN) + \mathcal{N}(FN) + \mathcal{N}(FP)}, \quad (18)$$

where we have used $\mathcal{N}(Z)$ as the count of the content of the set Z. Accuracy is more informative about the overall performance of the binary detector than sensitivity and specificity [28]. The computation of the above measures for our example(s) will be based on a comparison of the true annotations of the data with those obtained from the detector model. The performance of the proposed data-driven tuning smoothing parameters are compared with one-dimensional known kernel smoothing parameters candidates, Smoothed cross-validation bandwidth selector (HSCV), Normal scale bandwidth selector (Hns) and Plug-in bandwidth selector (Hpi), implemented in the R package for kernel smoothing, "ks" [29]. The benchmark smooth parameter candidates are denoted as $\hat{h}_{scv}, \hat{h}_i, \hat{h}_{ns}$

for HSCV, Hns and Hpi respectively, in all the examples considered. For tuning parameters that generate matrices, in particular, $\delta_i^1, \delta_i^2, \delta_i^3, \delta_i^4, \delta_i^{13}$ and δ_i^{14}, it is possible to obtain region of saturation as well as multiple highest performance statistics. Thus, in such cases, the best performance will be centered on averages of highest performance measures, using accuracy as basis for selection.

4.1 Physiological vital sign data application

We illustrate the utility of the proposed methods to public health problems. We consider the detection of normal vital signs measurements from a noisy physiological vital sign data set. A de-identified multivariate physiological vital sign data from Biofourmis Private Company Limited, Singapore is employed in this application. The data set is on physiological variables Systolic blood pressure (SBP), Diastolic blood pressure (DBP), Mean arterial pressure (MAP), Pulse Rate (PP), and Heart Rate (HR) with size 848×5. The data is from Singapore Heart Foundation (SINGHEART) study involving adult Asians in the age group $25 - 62$ years. Vital signs measurements were measured continuously from the subjects following different physiological states such as sleeping, walking, performing activities, etc. Table 2 provides a summary of the data. Figure 1 gives an overview of the nature of the vital signs in terms of distribution and the underlying inter-relationships existing among them, measured using Pearson correlation. The skewness of the physiological vital signs is illustrated as expected in any real physiological vital sign observed with context (physiological status eg. activity level etc.) taken into account.

Table 2. Summary statistics of physilogical vital signs.

	Vital sign				
Statistic	SBP	DBP	MAP	PP	HR
Minimum	78.00	44.00	55.00	20.00	45.00
Maximum	164.00	118.00	131.00	79.00	128.00
Mean	114.20	72.80	86.43	41.40	71.69
Median	114.00	73.00	86.00	41.00	72.00
Mode	116.0	71.0	89.0	42.0	75.0
sd	13.89	11.38	10.69	9.99	11.05
Skewness (η_3)	0.154	0.064	0.211	0.390	0.191

First, we explore some features of the statistics employed in the development of data-driven tuning proposals. The nature of the data-driven statistics ω_{1i}, ω_{i2} and $c(y)$ in relation with the estimated probability density function of the systolic blood pressure data is shown in Figure 2. The density feature preserving capability of the statistic, $c(y)$ is clearly evident. Also, the intrinsic differences among the ω_{1i} and ω_{2i} in terms of the observed systolic blood pressure structure underlying the data are clearly exhibited.

Figure 3 shows a plot of observational level tuning parameter estimates, δ_4^i, δ_5^i and δ_6^i against the systolic blood pressure observations. It can be seen that some data tuning parameters inherit the nature of the underlying probability density function of the data.

Figure 4 presents a sample relationship existing among common tuning parameter estimates, δ_8, δ_9 and δ_{10} and the systolic blood pressure measurement. The typical characteristics of δ_i^2 for four different values of α is illustrated in Figure 5. Figure 6 establishes

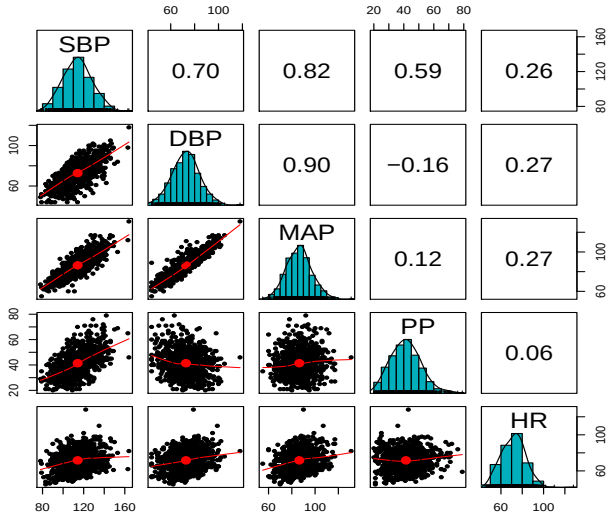

Figure 1. Nature of vital signs data showing densities, inter-relationships and pearson correlation coefficients.

the relationship between the statistic, ω_{i2} and each δ_1 and δ_2.

Figure 7 shows the nature of the observation-level tuning parameters,$\delta_i^1, \delta_i^2, \delta_i^3, \delta_i^4, \delta_i^{13}$ and δ_i^{14} defined by the systolic blood pressure data set, for three randomly selected candidates in each case.

Second, we examine the detection performance characteristics of the smoothing parameters with common data tuning. Figure 8 shows the dynamic performance nature of the proposed data-driven smoothing parameters with common tuning based on δ_g. It can be observed that lower values of δ_g support better performance in detection of normal systolic blood pressure with some smoothing parameters. In particular, $h^{\delta}{}_{c_4}$ gives superior performance over h_{c_1}, $h_{c_2}^{\delta}$ and $h_{c_3}^{\delta}$ for δ_g in the range $0.1 - 0.72$. Also, for higher values of δ_g, particularly, $\delta_g \in (0.73, 1.00)$, $h_{c_1}^{\delta}$ and $h_{c_3}^{\delta}$ consistently exhibit the same performances features. In general, $h_{c_1}^{\delta}$, $h_{c_3}^{\delta}$ yield the same increasing performance trend over the range of δ_g values.

Figure 9 shows the sensitivity, specificity, accuracy and F ratio plots against δ_1 for $h_{c_1}^{\delta}$, $h_{c_2}^{\delta}$, $h_{c_3}^{\delta}$ and $h_{c_4}^{\delta}$ with δ_1 as a tuning parameter. Clearly $h_{c_2}^{\delta}$ consistently results in better detection performance $(\text{SS} = 0.74, \text{SP} = 0.97, \text{ACC} = 0.92, \text{FR} = 0.96)$ than $h_{c_1}^{\delta}$, $h_{c_2}^{\delta}$ and $h_{c_3}^{\delta}$ for large values of δ_1, $(0.0285 \leq \delta_1 \leq 0.036)$.

The performance characteristics of $h_{c_1}^{\delta}$, $h_{c_2}^{\delta}$, $h_{c_3}^{\delta}$ and $h_{c_4}^{\delta}$ in model-based detection of normal systolic blood pressure measurement, when tuned with δ_2 are shown in Figure 10. From left to right are the plots for sensitivity, specificity, accuracy and F ratio. Though, $h_{c_2}^{\delta}$, and $h_{c_4}^{\delta}$ exhibit similar outstanding performance pattern with convergence at some values of δ_2, $h_{c_2}^{\delta}$ out performs $h_{c_4}^{\delta}$ on the average. It can be observed that $h_{c_2}^{\delta}$ yields optimal performance $(\text{SS} = 0.98, \text{SP} = 1.00, \text{ACC} = 0.97, \text{FR} = 0.94)$, for $0.095 \leq \delta_2 \leq 0.114$.

Table 3 reports the performance results for $h_{c_1}^{\delta}$ in comparison with h_i, h_{ns} and h_{csv}. $h_{c_1}^{\delta}$ achieves better performance than h_i, h_{ns} and h_{csv}, when not tuned ($\delta = 1$) and tuned using $\delta_3, \delta_4, \delta_5, \delta_6, \delta_7, \delta_8$, and δ_9. It can be seen that tuning is appropriate with the use of $h_{c_1}^{\delta}$ and in particular, δ values $(0.2641,\ 0.3049)$ that ensure small data tuning yield significant improvement in performance over large values. Furthermore, $h_{c_1}^{\delta}$ gives improved performance when used with δ_6 and δ_7 over h_i, h_{ns} and h_{csv}. However, $h_{c_1}^{\delta}$ is compatible with δ_7, yielding optimal performance over δ_6 across sensitivity, specificity, accuracy,

and FR ratio (SS $= 0.87$, SP $= 1.00$, ACC $= 0.97$, FR $= 0.93$).
Table 4 presents the performance statistics of $h_{c_2}^{\delta}$ for both tuned and non-tuned data cases. Again, an improvement in performance over the standard smoothing parameters, h_i, h_{ns} and h_{csv}, results when $h_{c_2}^{\delta}$ is tuned with $\delta_5, \delta_6, \delta_7, \delta_8$ and δ_9, corresponding to data tuning in the range $0.26 - 0.74$ The best performance for $h_{c_2}^{\delta}$ is obtained with δ_5, δ_6 and δ_7. Thus, $h_{c_1}^{\delta}$ adapts appropriately to the SBP data when tuned within $(0.26 - 0.56)$.
The improvement in performance offered by $h_{c_3}^{\delta}$ when used with the various tuning proposals is shown in Table 5. $h_{c_3}^{\delta}$ reports better performance over its counterparts, h_i, h_{ns} and h_{csv}, for $\delta = 1$, with SS $= 0.89$, SP $= 1.00$, ACC $= 0.97$, FR $= 0.94$, $\delta = \delta_7$, with SS $= 0.83$, SP $= 0.97$, ACC $= 0.94$, FR $= 0.86$, $\delta = \delta_8$, with SS $= 0.83$, SP $= 1.00$, ACC $= 0.96$, FR $= 0.91$, and $\delta = \delta_9$ with performance measures SS $= 0.83$, SP $= 0.97$, ACC $= 0.94$, FR $= 0.86$. Interestingly, the optimal performance for $h_{c_3}^{\delta}$ is obtained with δ set to 1. This suggest that $h_{c_3}^{\delta}$ is best if not tuned. However, the loss in performance associated with tuning with some δs for example δ, is significant.
Table 6 gives the performance of $h_{c_4}^{\delta}$ in comparison with h_i, h_{ns} and h_{csv}. It is easily seen that $h_{c_4}^{\delta}$ is better with $\delta = 1$, $\delta_5, \delta_6, \delta_7, \delta_8$ and δ_9 than h_i, h_{ns} and h_{csv}. Thus, $h_{c_4}^{\delta}$ yields significant improvement in performance when tuned with $\delta_5, \delta_6, \delta_7, \delta_8$ and δ_9. However, δ_7 stands out as the best data tuner for h_{c_4}, yielding the optimal performance result (SS $= 093.$, SP $= 1.00$, ACC $= 0.98$, FR $= 0.96$). It is clearly obvious that $h_{c_4}^{\delta}$ adapts best to the SBP data for self-normal detection for data tuners ensuring effective tuning in the range $0.26 - 0.56$.

Next, we examine the performance characteristics of the data-driven smoothing parameter estimators with adaptive weights. Figure 11, Figure 12, Figure 13, Figure 14, Figure 15 and Figure 16 show the performance statistics of h_v^2, h_v^3 and h_v^4 when tuned with $\delta_i^1, \delta_i^2, \delta_i^3, \delta_i^4, \delta_i^{13}$ and δ_i^{14}. The varying nature of the performance pattern among the smoothing parameters in relation with the tuning parameters is clearly evident. It can also be observed that some level of sensitivity exists among the tuning parameters. These saturation point(s) or region(s) especially, those associated with the best (highest) performance statistics provide valuable information for the selection of appropriate smoothing parameter estimate and its corresponding optimal tuning parameter value.
Table 8 gives the performance statistics of h_v^1 for the range of compatible tuning parameters, $\delta_i^8, \delta_i^9, \delta_i^{10}$ and δ_i^{12}. Clearly, h_v^1 results in significant improvement in performance over h_i, h_{ns} and h_{csv}. In particular, h_v^1 used with δ_i^8, δ_i^9 and δ_i^{11} yields improved performance statistics of the same magnitude with $(SS) = 0.83$, SP $= 0.97$, ACC $= 0.94$, and FR $= 0.86$.
Table 7 reports the performance of h_v^2 when utilized with, $\delta_i^1, \delta_i^2, \ldots, \delta_i^{14}$. Significant improvement in performance is obtained for all the appropriate tuners, $\delta_i^{1^*}, \delta_i^{2^*}, \delta_i^{3^*}, \delta_i^{4^*}, \delta_i^{5^*}, \delta_i^{6^*}, \delta_i^{7^*}, \delta_i^{13^*}, \delta_i^{14^*}$, associated with h_v^2. The δ_i^*s with the corresponding results are average values computed from the highest performance statistics obtained from the region of best performance with respect to accuracy. Apparently, though, h_v^2 is compatible with all the above tuning parameters, it is better with $\delta_i^{2^*}$, $\delta_i^{3^*}$, $\delta_i^{4^*}$, δ_i^5, δ_i^6, δ_i^7, δ_i^{13} and $\delta_i^{14^*}$. Nevertheless, it adapt best to the physiological dynamics associated with the systolic blood pressure measurement with $\delta_i^{3^*}$, $\delta_i^{7^*}$ and $\delta_i^{14^*}$.
Table 8 gives the performance statistics of h_v^3 for the set of appropriate data-drive tuners. h_v^3 adapts better to the data when used with $\delta_i^{2^*}$, δ_i^5, δ_i^6, δ_i^7, δ_i^8, δ_i^9, δ_i^{11}, yielding significant improvement in performance over h_i, h_{ns} and h_{csv}. Optimal adaptation resulting in best performance for h_v^3 are obtained when it is used with δ_i^7 and δ_i^8.
Table 8 presents the performance results for h_i^4 over the range compatible tuners δ_i. It can be see that δ_i^6, δ_i^8, δ_i^9, δ_i^{11} and δ_i^{13} ensure better adaption of h_v^4 to the data, resulting in an improved performance over the known counterparts, h_i, h_{ns} and h_{csv}. However, δ_i^8 gives the best adaption, resulting in the optimal performance with accuracy value of 0.98.
Table 11 presents the optimal performance statistics of $h_{c_1}^{\delta}$, $h_{c_2}^{\delta}$, $h_{c_3}^{\delta}$, $h_{c_4}^{\delta}, h_v^1$, h_v^2, h_v^3, and h_v^4 with their corresponding compatible data tuners. The flexibility associated with the proposed smoothing parameters in terms of their capability to couple or blend with multiple data-driven tuners is clearly evident.
Table 12 reports the summary of the best tuning required for each of $h_{c_1}^{\delta}$, $h_{c_2}^{\delta}$, $h_{c_3}^{\delta}$, $h_{c_4}^{\delta}, h_v^1$, h_v^2, h_v^3, and h_v^4 to adapt sufficiently to the SBP data for improved performance. It can be observed that some level of tuning is required for almost all the above proposals to yield improvement in performance. The level tuning appropriate for each smoothing parameter is specific and dependent on structure and design of δ. Also, $h_{c_1}^{\delta_7}$, $h_{c_2}^{\delta_5}$, $h_{c_2}^{\delta_6}$, and $h_{c_3}^{\delta=1}$ yield the same optimal performance statistics (ACC $= 0.97$). Nevertheless, $h_{c_4}^{\delta_7}$ outperforms $h_{c_1}^{\delta_7}$, $h_{c_2}^{\delta_5}$, $h_{c_2}^{\delta_6}$, and $h_{c_3}^{\delta=1}$ with the optimal accuracy value of 0.98. Although,$(h_v^2, \delta_i^{3^*})$, (h_v^2, δ_i^7), $(h_v^2, \delta_i^{14^*})$, (h_v^3, δ_i^7), (h_v^3, δ_i^8) and (h_v^4, δ_i^7) exhibit the same optimal performance characteristics, each outperforms $h_{c_1}^{\delta_7}$, $h_{c_2}^{\delta_5}$, $h_{c_2}^{\delta_6}$, $h_{c_3}^1$, h_v^1 with both δ_i^8 and δ_i^9. Here, we have written (h_v^j, δ_i^k) to mean h_v^j tuned (used) with δ_i^k. Furthermore, the difference in improvement offered by the entire data and observation level tuning can be clearly seen with the latter yielding significant improvement in performance, in general.

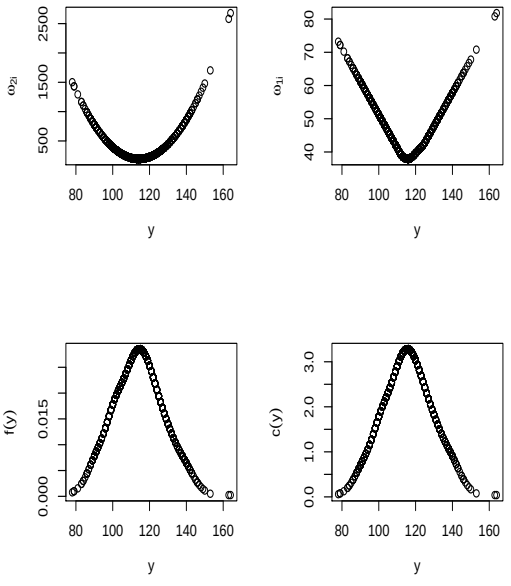

Figure 2. Nature of estimated kernel density of data and its derived weigths, ω_{1i} and ω_{2i}

.

5 Conclusion

In this paper, we have proposed and implemented novel tunable data-driven smoothing parameter estimators with various tuning schemes for performing non-parametric normal systolic blood pressure detection from training data. The tuning schemes are based on common

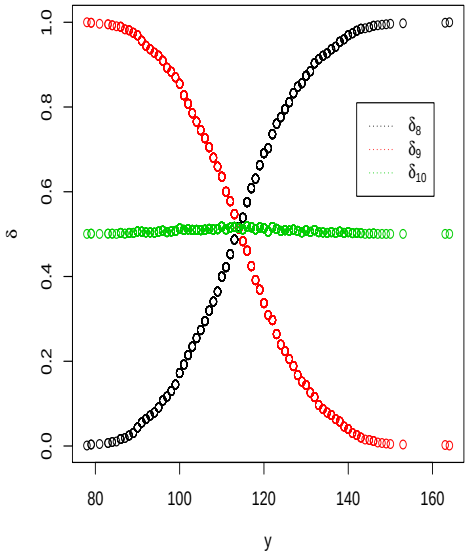

Figure 3. Nature of data dependent weights.

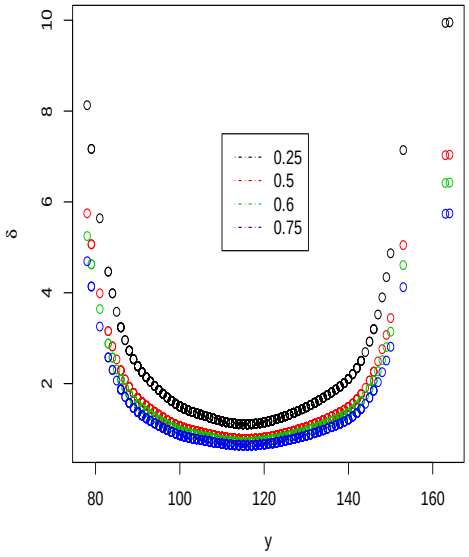

Figure 5. Plot of data against δ_{12}^i for α values $0.25, 0.5, 0.6$ and 0.75.

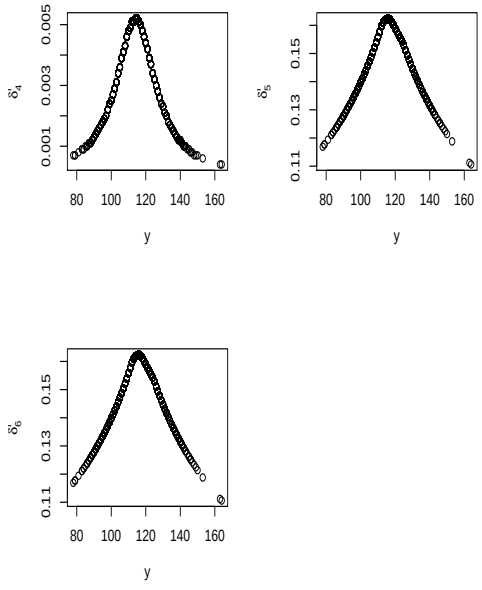

Figure 4. Plot of data against tuning parameters, δ_4^i, δ_5^i and δ_6^i.

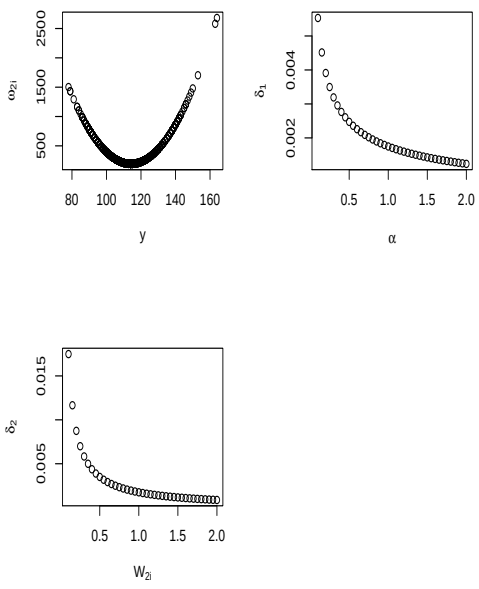

Figure 6. Nature of statistic, ω_{2i} in relation with δ_1 and δ_2.

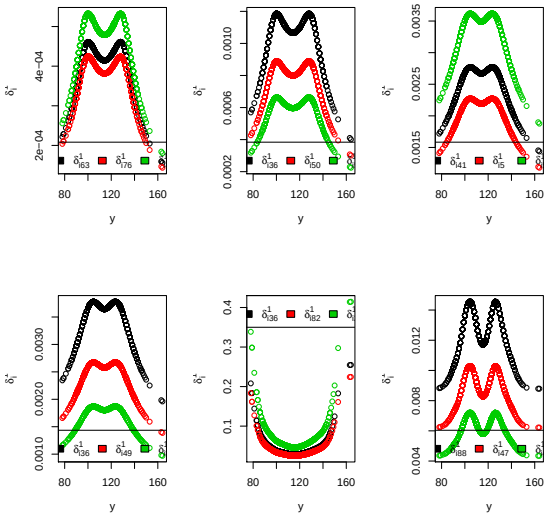

Figure 7. Graph of δ_is; $\delta_i^1, \delta_i^2, \delta_i^3, \delta_i^4, \delta_i^{13}$ and δ_i^{14}. against systolic blood pressure, y.

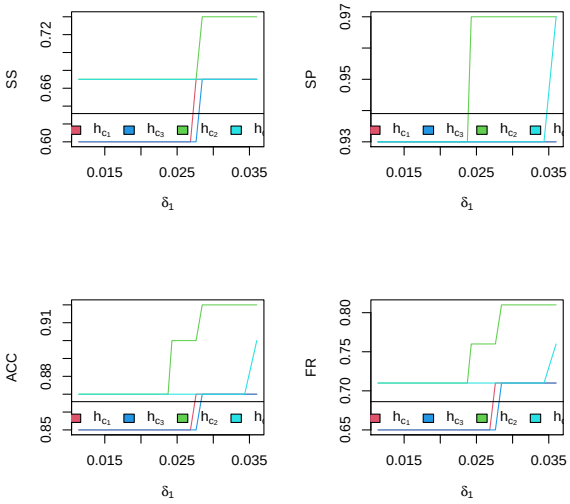

Figure 9. Performance of $h_{c_1}, h_{c_2}, h_{c_3}$ and h_{c_4} with δ_1.

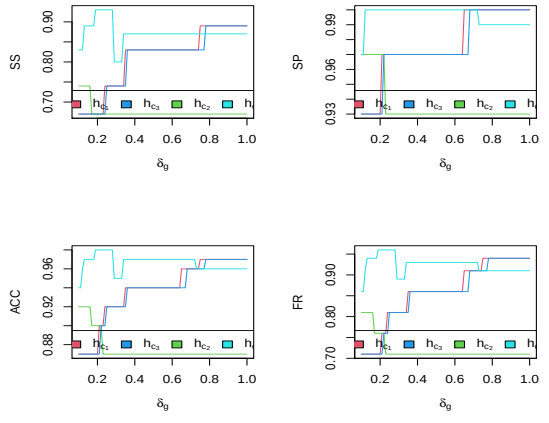

Figure 8. Performance of $h_{c_1}, h_{c_2}, h_{c_3}$ and h_{c_4} with δ_g.

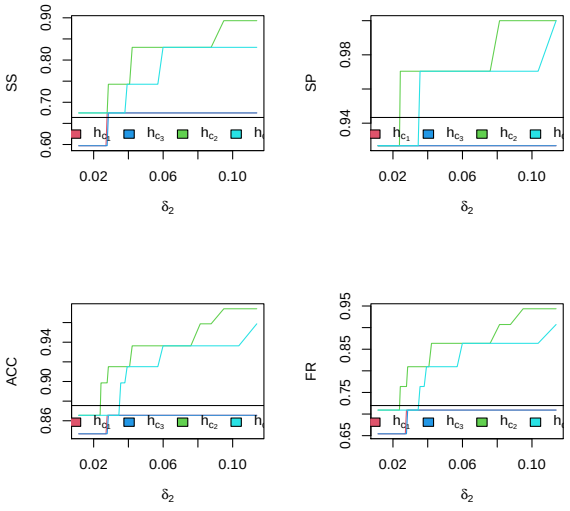

Figure 10. Performance of $h_{c_1}, h_{c_2}, h_{c_3}$ and h_{c_4} with δ_2.

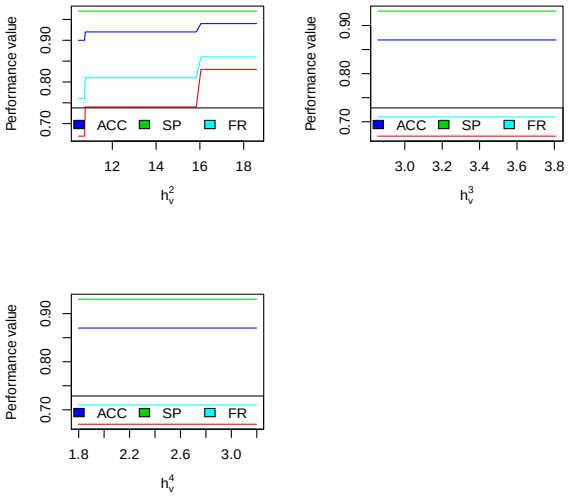

Figure 11. Graph of performance statistics ofh_v^2, h_v^3 and h_v^4 with δ_i^1. Red lines=SS, green lines=SP,blue lines=ACC and sea blue lines=FR.

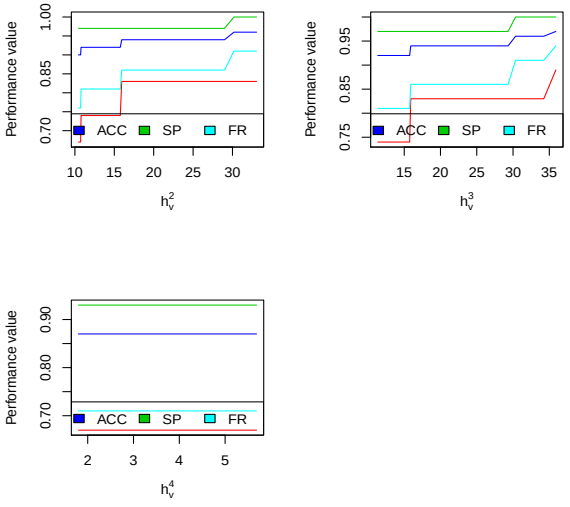

Figure 12. Graph of performance statistics of h_v^2, h_v^3 and h_v^4 with δ_i^2. Red lines=SS, green lines=SP,blue lines=ACC and sea blue lines=FR.

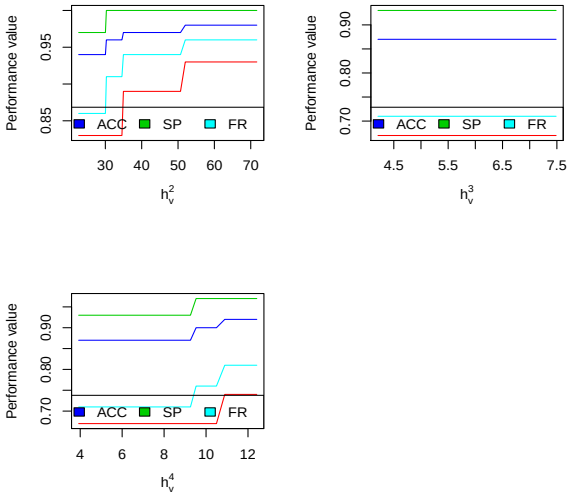

Figure 13. Graph of performance statistics of $\hat{h}_v^2, \hat{h}_v^3$ and $\hat{h}_v^4$ with δ_i^3. Red lines=SS, green lines=SP, blue lines=ACC and sea blue lines=FR.

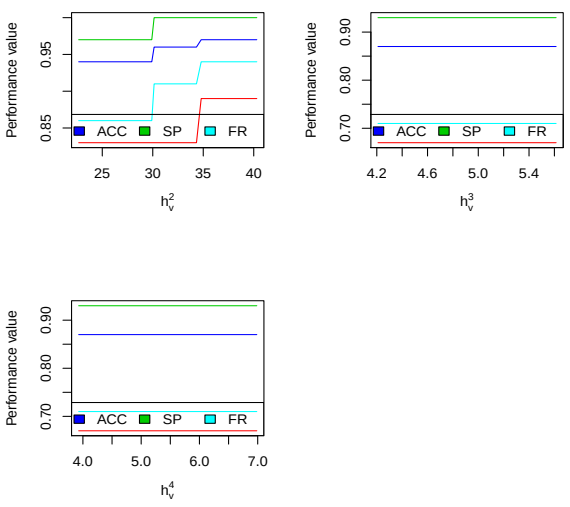

Figure 14. Graph of performance statistics of h_v^2, h_v^3 and h_v^4 with δ_i^4. Red lines=SS, green lines=SP, blue lines=ACC and sea blue lines=FR.

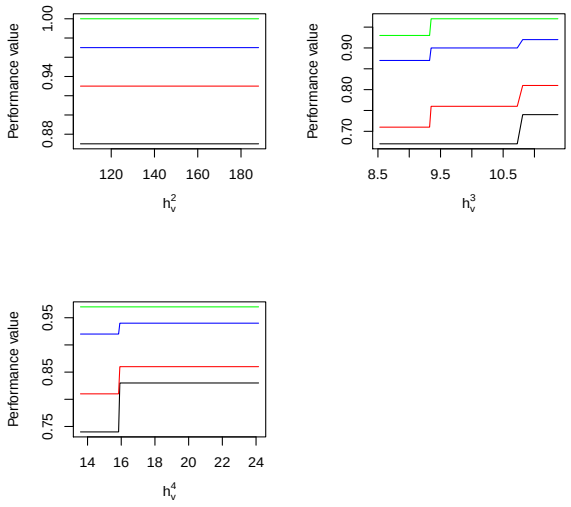

Figure 15. Graph of performance statistics of h_v^2, h_v^3 and h_v^4 with δ_i^{13}

		$h_{c_1}^{\delta}$				
δ	$\hat{\delta}$	$\hat{h}_{c_1}^{\delta}$	SS	SP	ACC	FR
δ	1.0000	46.342	0.75	0.96	0.91	0.80
δ_3	0.0137	0.634	0.60	0.88	0.81	0.60
δ_4	0.0106	0.492	0.60	0.88	0.81	0.60
δ_5	0.4835	22.406	0.75	0.96	0.91	0.80
δ_6	0.3049	14.129	0.87	0.99	0.96	0.91
δ_7	0.2641	12.24	0.87	1.00	0.97	0.93
δ_8	0.7387	34.23	0.75	0.96	0.91	0.80
δ_9	0.5556	25.748	0.75	0.96	0.91	0.80
$\hat{h}_i$		3.84	0.74	0.97	0.92	0.81
$\hat{h}_{\text{ns}}$		3.82	0.74	0.97	0.92	0.81
$\hat{h}_{\text{scv}}$		3.87	0.74	0.97	0.92	0.81

Table 3. Performance statistics of $h_{c_1}^{\delta}$ over range of δ. SS=Sensitivity, SP=Specificity, ACC=Accuracy, FR=F-ratio.

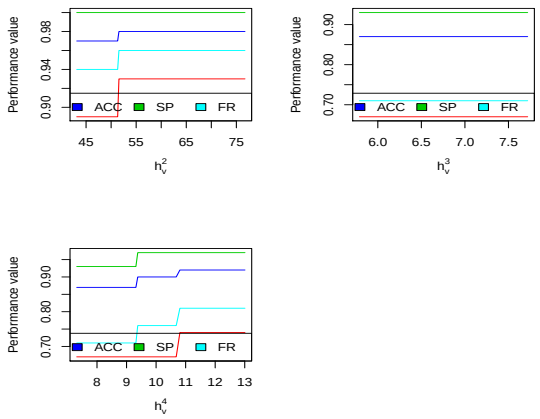

Figure 16. Graph of performance statistics of $\hat{h}_v^2, \hat{h}_v^3$ and $\hat{h}_v^4$ with δ_i^{14}. Red lines=SS, green lines=SP, blue lines=ACC and sea blue lines=FR.

		$h_{c_2}^{\delta}$				
δ	$\hat{\delta}$	$\hat{h}_{c_2}^{\delta}$	SS	SP	ACC	FR
δ	1.0000	19.648	0.75	0.99	0.93	0.84
δ_3	0.0137	2.299	0.67	0.93	0.87	0.71
δ_4	0.0106	2.025	0.67	0.93	0.87	0.71
δ_5	0.4835	13.662	0.87	1.00	0.97	0.93
δ_6	0.3049	10.849	0.87	1.00	0.97	0.93
δ_7	0.2641	10.098	0.87	1.00	0.97	0.93
δ_8	0.7387	16.886	0.75	0.99	0.93	0.84
δ_9	0.5556	14.646	0.87	0.99	0.96	0.91
$\hat{h}_i$		3.84	0.74	0.97	0.92	0.81
$\hat{h}_{\text{ns}}$		3.82	0.74	0.97	0.92	0.81
$\hat{h}_{\text{scv}}$		3.87	0.74	0.97	0.92	0.81

Table 4. Performance statistics of $h_{c_2}^{\delta}$ over range of δ. SS=Sensitivity, SP=Specificity, ACC=Accuracy, FR=F-ratio.

		$h^{\delta}_{c_3}$				
δ	$\hat{\delta}$	$\hat{h}^{\delta}_{c_3}$	SS	SP	ACC	FR
δ	1.0000	6.662	0.89	1.00	0.97	0.94
δ_3	0.0137	0.779	0.60	0.93	0.85	0.65
δ_4	0.0106	0.687	0.60	0.93	0.85	0.65
δ_5	0.4835	4.632	0.83	0.97	0.94	0.86
δ_6	0.3049	3.678	0.74	0.97	0.92	0.81
δ_7	0.2641	3.424	0.74	0.97	0.92	0.81
δ_8	0.7387	5.725	0.83	1.00	0.96	0.91
δ_9	0.5556	4.966	0.83	0.97	0.94	0.86
$\hat{h}_i$		3.84	0.743	0.97	0.92	0.81
$\hat{h}_{\text{ns}}$		3.82	0.74	0.97	0.92	0.81
$\hat{h}_{\text{scv}}$		3.87	0.74	0.97	0.92	0.81

Table 5. Performance statistics of $h^{\delta}_{c_3}$ over range of δ. SS=Sensitivity, SP=Specificity, ACC=Accuracy, FR=F-ratio.

		$h^{\delta}_{c_4}$				
δ	$\hat{\delta}$	$\hat{h}^{\delta}_{c_4}$	SS	SP	ACC	FR
δ	1.0000	16.492	0.87	0.99	0.96	0.91
δ_3	0.0137	2.000	0.67	0.93	0.87	0.71
δ_4	0.0106	1.732	0.67	0.93	0.87	0.71
δ_5	0.4835	11.446	0.87	1.00	0.97	0.93
δ_6	0.3049	9.110	0.80	1.00	0.95	0.89
δ_7	0.2641	8.485	0.93	1.00	0.98	0.96
δ_8	0.7387	14.177	0.87	0.99	0.96	0.91
δ_9	0.5556	12.288	0.87	1.00	0.97	0.93
$\hat{h}_i$		3.84	0.74	0.97	0.92	0.81
$\hat{h}_{\text{ns}}$		3.82	0.74	0.97	0.92	0.81
$\hat{h}_{\text{scv}}$		3.87	0.74	0.97	0.92	0.81

Table 6. Performance statistics of $h^{\delta}_{c_4}$ over range of δ. SS=Sensitivity, SP=Specificity, ACC=Accuracy, FR=F-ratio.

	h^1_v				
δ_i	$\hat{h}^1_v$	SS	SP	ACC	FR
δ^8_i	23.1067	0.83	0.97	0.94	0.86
δ^9_i	24.1612	0.83	0.97	0.94	0.86
δ^{10}_i	4.3748	0.67	0.93	0.87	0.71
δ^{11}_i	29.8449	0.83	0.97	0.94	0.86
δ^{12}_i	3.9406	0.67	0.93	0.87	0.71

Table 7. Performance statistics of $\hat{h}^1_v$ over the δ_is. SS=Sensitivity, SP=Specificity, ACC=Accuracy, FR=F-ratio.

	$\hat{h}^2_v$				
δ_i	$\hat{h}^2_v$	SS	SP	ACC	FR
δ^{1*}_i	17.185	0.83	0.97	0.94	0.86
δ^{2*}_i	18.168	0.83	1.00	0.96	0.91
δ^{3*}_i	60.442	0.93	1.00	0.98	0.96
δ^{4*}_i	37.256	0.89	1.00	0.97	0.94
δ^5_i	31.920	0.83	1.00	0.96	0.91
δ^6_i	134.321	0.87	1.00	0.97	0.93
δ^7_i	56.400	0.93	1.00	0.98	0.96
δ^{13*}_i	129.058	0.87	1.00	0.97	0.93
δ^{14*}_i	60.255	0.93	1.00	0.98	0.96

Table 8. Performance statistics of $\hat{h}^2_v$ over the δ_is. SS=Sensitivity, SP=Specificity, ACC=Accuracy, FR=F-ratio. Values with $*$ are averages of optimal performance statistics based on ACC, within a region of saturation.

	h_v^3				
δ_i	$\hat{h}_v^3$	SS	SP	ACC	FR
δ_i^{1*}	3.145^*	0.67	0.93	0.87	0.71
δ_i^{2*}	3.808^*	0.89	1.00	0.97	0.94
δ_i^{3*}	5.135^*	0.67	0.93	0.87	0.71
δ_i^{4*}	4.636^*	0.67	0.93	0.87	0.71
δ_i^5	34.908	0.89	1.00	0.97	0.94
δ_i^6	145.402	0.87	1.00	0.97	0.93
δ_i^7	61.263	0.93	1.00	0.98	0.96
δ_i^8	67.537	0.93	1.00	0.98	0.96
δ_i^9	24.161	0.83	0.97	0.94	0.86
δ_i^{10}	4.375	0.67	0.93	0.87	0.71
δ_i^{11}	29.845	0.83	0.97	0.94	0.86
δ_i^{12}	3.941	0.67	0.93	0.87	0.71
δ_i^{13*}	11.077^*	0.74	0.97	0.92	0.81
δ_i^{14*}	6.375^*	0.67	0.93	0.87	0.71

Table 9. Performance statistics of $\hat{h}_v^2$ over the δ_is. SS=Sensitivity, SP=Specificity, ACC=Accuracy, FR=F-ratio. Values with $*$ are averages of optimal performance statistics based on ACC, within a region of saturation.

	h_v^4				
δ_i	$\hat{h}_v^4$	SS	SP	ACC	FR
δ_i^{1*}	2.194^*	0.67	0.93	0.87	0.71
δ_i^{2*}	2.194^*	0.67	0.93	0.87	0.71
δ_i^{3*}	11.623^*	0.74	0.97	0.92	0.81
δ_i^{4*}	4.791^*	0.67	0.93	0.87	0.71
δ_i^5	5.584	0.67	0.93	0.87	0.71
δ_i^6	22.847	0.83	0.97	0.94	0.86
δ_i^7	9.703	0.67	0.97	0.90	0.76
δ_i^8	67.537	0.93	1.00	0.98	0.96
δ_i^9	24.161	0.83	0.97	0.94	0.86
δ_i^{10}	4.375	0.67	0.93	0.87	0.71
δ_i^{11}	29.845	0.83	0.97	0.94	0.86
δ_i^{12}	3.941	0.67	0.93	0.87	0.71
δ_i^{13*}	18.701^*	0.83	0.97	0.94	0.86
δ_i^{14*}	11.754^*	0.74	0.97	0.92	0.81

Table 10. Performance statistics of $\hat{h}_v^4$ over the δ_is. SS=Sensitivity, SP=Specificity, ACC=Accuracy, FR=F-ratio. Values with $*$ are averages of optimal performance statistics based on ACC, within a region of saturation.

	$h_{c_1}^\delta, h_{c_2}^\delta, h_{c_3}^\delta, h_{c_4}^\delta, \hat{h}_v^1, h_v^2, h_v^3, h_v^4$				
h^δ	δ	SS	SP	ACC	FR
$h_{c_1}^\delta$	δ_7	0.87	1.00	0.97	0.93
$h_{c_2}^\delta$	$\delta_5, \delta_6, \delta_7$	0.87	1.00	0.97	0.93
$h_{c_3}^\delta$	δ_g $(\delta_g = 1.00)$	0.89	1.00	0.97	0.94
$h_{c_3}^\delta$	δ_8	0.83	1.00	0.96	0.91
$h_{c_4}^\delta$	δ_7	0.93	1.00	0.98	0.96
h_v^1	$\delta_i^8, \delta_i^9, \delta_i^{11}$	0.83	0.97	0.94	0.86
h_v^2	$\delta_i^{3*}, \delta_i^7, \delta_i^{14*}$	0.93	1.00	0.98	0.96
h_v^3	δ_i^7, δ_i^8	0.93	1.00	0.98	0.96
h_v^4	δ_i^8	0.93	1.00	0.98	0.96

Table 11. Optimal performance statistics of smoothing parameters with best data tuning parameters. SS=Sensitivity, SP=Specificity, ACC=Accuracy, FR=F-ratio.

	$h_{c_1}^\delta, h_{c_2}^\delta, h_{c_3}^\delta, h_{c_4}^\delta, h_v^1, h_v^2, h_v^3, h_v^4$			
h^δ	δ	$\hat{\delta}$	$\hat{h}^\delta$	ACC
$h_{c_1}^\delta$	δ_7	0.264	12.240	0.97
$h_{c_2}^\delta$	δ_5	0.484	13.662	0.97
$h_{c_2}^\delta$	δ_6	0.305	10.849	0.97
$h_{c_2}^\delta$	δ_7	0.264	10.098	0.97
$h_{c_3}^\delta$	δ_g	1.000	6.662	0.97
$h_{c_3}^\delta$	δ_8	0.739	5.725	0.96
$h_{c_4}^\delta$	δ_7	0.264	8.485	0.98
h_v^1	δ_i^8		23.107	0.94
h_v^1	δ_i^9		24.161	0.94
h_v^1	δ_i^{11}		29.845	0.94
h_v^2	δ_i^{3*}		60.442	0.98
h_v^2	δ_i^7		56.400	0.98
h_v^2	δ_i^{14*}		60.255	0.98
h_v^3	δ_i^7		61.263	0.98
h_v^3	δ_i^8		67.537	0.98
h_v^4	δ_i^7		67.537	0.98

Table 12. Best data tuning parameters with their corresponding estimate of h.

(entire data) or observation-specific weighting, using bye-products of the developed statistics for normal data detection. Application to real systolic blood pressure data set shows that data tuning allows adaptation of smoothing parameters to the intrinsic structures underlying the training data for improved performance. Furthermore, observation specific tuning offer substantial improvement in performance than the entire data tuning. In particular, the smoothing parameters, $h_{c_1}^{\delta_7}$, $h_{c_2}^{\delta_5}$, $h_{c_2}^{\delta_6}$, $h_{c_2}^{\delta_7}$, $h_{c_3}^{\delta_8}$ each yielded 5% improvement (h_v^1, δ_i^8), (h_v^1, δ_i^9) and $\delta_i^{11})$ resulted in 2% improvement; $h_{c_4}^{\delta_7}, (h_v^2, \delta_i^{3*})$, (h_v^2, δ_i^7), (h_v^2, δ_i^{14*}), (h_v^3, δ_i^7), (h_v^3, δ_i^8) and (h_v^4, δ_i^{3*}), each yielded 6% improvement in overall performance based on accuracy over the smoothed cross-validation bandwidth selector (HSCV), normal scale bandwidth selector (Hns) and Plug-in bandwidth selector (Hpi), for a univariate data. Although, current interest is centered on accuracy as overall performance assessment, various problem-specific detection solutions can be designed. For example, solution(s) based on sensitivity and specificity can be considered for which most of the tuning proposals are evidently up-to the task.

Funding

This research was funded by the Directorate of Research Innovation and Consultancy (DRIC), University of Cape Coast, with the Special Research Support grant RSG/INDI/CANS/2020/131.

Acknowledgment

The authors gratefully acknowledge the support of the Speicial Research Grant RSG/INDI/CANS/2020/131 from the Directorate of DRIC, University of Cape Coast, and Biofourmis Private Company Limited, Singapore with real physiological vital signs data set. Finally, we greatly appreciate the editor, supporting staff of HRPUB, and reviewers for their help and constructive comments that improved the style and substance of the paper.

REFERENCES

[1] M. D. Buist, P. R. Burton, S. A. Bernard, B. P. Waxman, and J. Anderson, "Recognising clinical instability in hospital patients before cardiac arrest or unplanned admission to intensive care: A pilot study in a tertiary-care hospital," *Medical Journal of Australia*, vol. 171, no. 1, pp. 22–25, 1999.

[2] D. Evans, B. Hodgkinson, and J. Berry, "Vital signs in hospital patients: a systematic review," *International journal of nursing studies*, vol. 38, no. 6, pp. 643–650, 2001.

[3] C. for Clinical Practice at NICE (UK *et al.*, "Acutely ill patients in hospital: recognition of and response to acute illness in adults in hospital," 2007.

[4] J. Gardner-Thorpe, N. Love, J. Wrightson, S. Walsh, and N. Keeling, "The value of modified early warning score (mews) in surgical in-patients: a prospective observational study," *The Annals of The Royal College of Surgeons of England*, vol. 88, no. 6, pp. 571–575, 2006.

[5] S. Khalid, D. A. Clifton, and L. Tarassenko, "A bayesian patient-based model for detecting deterioration in vital signs using manual observations," in *International Symposium on Foundations of Health Informatics Engineering and Systems*, pp. 146–158, Springer, 2013.

[6] M. Markou and S. Singh, "Novelty detection: a review—part 1: statistical approaches," *Signal processing*, vol. 83, no. 12, pp. 2481–2497, 2003.

[7] M. Markou and S. Singh, "Novelty detection: a review—part 2:: neural network based approaches," *Signal processing*, vol. 83, no. 12, pp. 2499–2521, 2003.

[8] M. A. Pimentel, D. A. Clifton, L. Clifton, P. J. Watkinson, and L. Tarassenko, "Modelling physiological deterioration in post-operative patient vital-sign data," *Medical & biological engineering & computing*, vol. 51, no. 8, pp. 869–877, 2013.

[9] C. Velardo, S. A. Shah, O. Gibson, H. Rutter, A. Farmer, and L. Tarassenko, "Automatic generation of personalised alert thresholds for patients with copd," in *Signal Processing Conference (EUSIPCO), 2014 Proceedings of the 22nd European*, pp. 1990–1994, IEEE, 2014.

[10] D. K. Mensah and S. A. F. Eyiah-Bediako, "On statistical approach to automated normal systolic blood pressure detection in continuously monitored blood pressure data," *Journal of Natural Sciences Research*, vol. 10, no. 4, 2020.

[11] M. C. Jones, J. S. Marron, and S. J. Sheather, "A brief survey of bandwidth selection for density estimation," *Journal of the American statistical association*, vol. 91, no. 433, pp. 401–407, 1996.

[12] D. W. Scott, *Multivariate density estimation: theory, practice, and visualization*. John Wiley & Sons, 2015.

[13] R. Stanton, "A nonparametric model of term structure dynamics and the market price of interest rate risk," *The Journal of Finance*, vol. 52, no. 5, pp. 1973–2002, 1997.

[14] S. G. Donald, "Inference concerning the number of factors in a multivariate nonparametric relationship," *Econometrica: Journal of the Econometric Society*, pp. 103–131, 1997.

[15] P. De Valpine, "Monte carlo state-space likelihoods by weighted posterior kernel density estimation," *Journal of the American Statistical Association*, vol. 99, no. 466, pp. 523–536, 2004.

[16] G. W. Colopy, T. Zhu, L. Clifton, S. J. Roberts, and D. A. Clifton, "Likelihood-based artefact detection in continuously-acquired patient vital signs," in *2017 39th Annual International Conference of the IEEE Engineering in Medicine and Biology Society (EMBC)*, pp. 2146–2149, IEEE, 2017.

[17] C. Velardo, S. A. Shah, O. Gibson, H. Rutter, A. Farmer, and L. Tarassenko, "Automatic generation of personalised alert thresholds for patients with copd," in *2014 22nd European Signal Processing Conference (EUSIPCO)*, pp. 1990–1994, IEEE, 2014.

[18] A. J. Izenman, "Review papers: Recent developments in nonparametric density estimation," *Journal of the American Statistical Association*, vol. 86, no. 413, pp. 205–224, 1991.

[19] J. S. Marron, "Automatic smoothing parameter selection: a survey," in *Semiparametric and nonparametric econometrics*, pp. 65–86, Springer, 1989.

[20] S. J. Sheather and M. C. Jones, "A reliable data-based bandwidth selection method for kernel density estimation," *Journal of the Royal Statistical Society: Series B (Methodological)*, vol. 53, no. 3, pp. 683–690, 1991.

[21] C. C. Taylor, "Bootstrap choice of the smoothing parameter in kernel density estimation," *Biometrika*, vol. 76, no. 4, pp. 705–712, 1989.

[22] C. M. Bishop, *Pattern recognition and machine learning*. springer, 2006.

[23] B. W. Silverman, *Density estimation for statistics and data analysis*, vol. 26. CRC press, 1986.

[24] R. A. Davis, K.-S. Lii, and D. N. Politis, "Remarks on some nonparametric estimates of a density function," in *Selected Works of Murray Rosenblatt*, pp. 95–100, Springer, 2011.

[25] R. A. Maronna, R. D. Martin, V. J. Yohai, and M. Salibián-Barrera, *Robust statistics: theory and methods (with R)*. John Wiley & Sons, 2019.

[26] F. Liu, X. Cheng, and D. Chen, "Insider attacker detection in wireless sensor networks," in *IEEE INFOCOM 2007-26th IEEE International Conference on Computer Communications*, pp. 1937–1945, IEEE, 2007.

[27] C. M. Bishop, "Novelty detection and neural network validation," *IEE Proceedings-Vision, Image and Signal processing*, vol. 141, no. 4, pp. 217–222, 1994.

[28] M. Vihinen, "How to evaluate performance of prediction methods? measures and their interpretation in variation effect analysis," in *BMC genomics*, vol. 13, p. S2, BioMed Central, 2012.

[29] T. Duong *et al.*, "ks: Kernel density estimation and kernel discriminant analysis for multivariate data in r," *Journal of Statistical Software*, vol. 21, no. 7, pp. 1–16, 2007.